




Removal of Particulates on the Fabric Surface and Evaluation by Image Processing

Se Young Yoon¹ · Kyungha Baik¹ · Suhyun Lee¹ · Chung Hee Park¹ 

Received: 3 February 2022 / Revised: 2 March 2023 / Accepted: 7 March 2023 / Published online: 12 April 2023
© The Author(s), under exclusive licence to the Korean Fiber Society 2023

Abstract

Three noncontact methods of evaluating the particle removal rate from fabrics were developed using image processing, and the dust particle removal rate by a clothing care machine was evaluated for the six fabric samples with different moisture characteristics and geometric structures. The removal rates calculated for the six samples showed a constant tendency, thereby confirming that the dust removal evaluation methods developed in this study have proved a reliability. It was also found that dust adhesion on the fabrics was affected by the surface structure rather than the moisture characteristics of the fibers, where more dust adhered to knitted fabrics than to woven fabrics. By contrast, the dust removal rate was higher for woven fabrics than for knitted fabrics, and the removal rate for woven polyester fabric, which had low hydrophilicity, was higher than those for woven cotton and wool fabrics. Furthermore, the removal rate tended to be high for samples with a low coefficient of friction. When particle removal during each step of the four-step dust removal course of the machine was evaluated, polyester fabrics had the highest removal rate in the step with high-humidity condition. However, the removal rate for cotton fabrics was the highest when they were treated under relatively low humidity with strong air flow.

Keywords Particle removal rate · Image processing · Clothing care machine · Moisture regain · Coefficient of friction

1 Introduction

Air pollution, one of the most serious environmental problems in modern society, can cause various diseases. According to the World Health Organization, air pollution was responsible for one of nine deaths in 2012. In particular, three million died from external air pollution. Particulate matter (PM) with diameters of 10 μm or less is known to be more harmful because it accumulates in the lungs without being discharged when inhaled into the human body [1].

PM is a mixture of solid and liquid organic or inorganic substances; their proportions may vary depending on the time and area of measurement and the size of PM. However, the main components of PM are known to be soluble components, such as sulfate (SO_4^{2-}), ammonium (NH_4^+), and nitrate (NO_3^-); insoluble components, such as organic

carbon, elemental carbon, and water. Depending on its size, PM is classified as PM₁₀ (diameters of 10 μm or less) and PM_{2.5} (diameters of 2.5 μm or less) [1, 2]. PM in the atmosphere is introduced to indoor spaces by adhering to clothing during long or frequent outdoor activities. The adhesion of PM to fabrics can be explained in terms of impingement and retention. Impingement is divided into direct contact with pollution sources and impingement on fabric surfaces via airborne or liquid-borne PM.

The adhesion of PM to fabrics through impingement via a fluid can also be explained by the filtration principle shown in Fig. 1 [3]. Macroscopically, PM in the atmosphere appears to exhibit linear motion, but microscopically, it travels by random movement through Brownian motion. PM particles adhere to fabric surfaces through actions, such as impaction, interception, and diffusion (Brownian motion), gravity, and electrostatic force. Interception occurs when the distance between a dust particle and a fabric (collector) becomes equal to or smaller than the particle radius as the particle moves along an airflow streamline around the collector. Inertial impaction occurs when a particle with a diameter of approximately 1 μm or larger in rapidly flowing

✉ Suhyun Lee
suhyun14@snu.ac.kr

Chung Hee Park
junghee@snu.ac.kr

¹ Department of Fashion and Textiles, Seoul National University, Seoul 08826, Korea

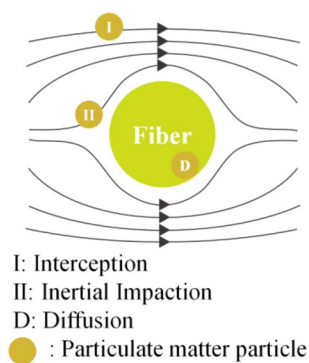


Fig. 1 Illustration of filter capture mechanism [3]

air escapes from an airflow streamline because of inertia and collides with a collector [4].

After impingement on a fabric, PM may be retained by mechanical forces, electrostatic forces, or oil bonding [5–7]. According to Compton and Hart [8], retention occurs through three mechanisms: macro-occlusion, in which particles are entrapped in the intra or inter yarn; micro-occlusion, in which particles are entrapped in irregular structures or shapes on the fabric surface; and sorption by van der Waals or Coulombic forces. In macro- or micro-occlusion, retention is caused by the shape and structure of the fiber, yarn, and fabric, including the space between yarns, space between fibers in a single yarn, curvature of the fiber such as the ribbon shape of cotton fibers, and surface microstructure such as wool scales or hair fibers. Dust particles trapped by macro-occlusion can be easily removed with mechanical force because the bond between the fabric and dust is weaker than that in micro-occlusion. By contrast, when sorption occurs, small particles can easily be retained in fabrics by van der Waals forces alone. Moreover, electrostatic forces may develop, depending on the moisture regain of the fiber.

PM attached to a fabric may leave a stain if it contacts a liquid and penetrates the fabric. For polar liquids in particular, the dissolved PM component is drawn deep into the fiber, causing serious staining and damage to clothing [5, 9, 10]. Therefore, it is important to promptly remove PM from clothing by physical and chemical methods.

In recent years, the electronics industry has developed and launched clothing care machines that remove pollutants, including PM, from contaminated clothing, restore deformed fabric, and perform deodorization and sterilization to make clothing management more convenient. Because PM removal, fabric deformation recovery, deodorization, and sterilization involve different mechanisms, they require different care processes and evaluation methods. However, there are no appropriate methods for the quantitative evaluation of PM removal by clothing care machines. Sensory tests or surface reflectance measurements have generally been

employed to evaluate the removal of particulate soil from clothing surfaces. Sensory tests are subjective but have low reproducibility. By contrast, surface reflectance measurement is objective, and the results are reproducible; however, because it is a contact-type measurement, it cannot be used to measure loosely bound dust on clothing surfaces. Therefore, it is necessary to develop an objective, quantitative noncontact measurement method of evaluating the removal rate of PM attached to clothing [11]. If the PM removal program in clothing care machines is adjusted according to the fabric characteristics based on this evaluation method, effective clothing management will be possible.

In this study, an objective, quantitative evaluation method for determining the removal rate of PM on fabric surfaces was developed using a noncontact image analysis method. The PM removal performance of a clothing care machine was evaluated to determine which factors among the environmental conditions in the clothing care machine affect dust removal. To this end, six fabrics woven or knitted of cotton, polyester, or wool fibers were employed, and the PM removal rates during the dust removal course of the clothing care machine were evaluated. The dust removal rate was then analyzed according to the moisture regain, coefficient of friction, and surface roughness of each material. In addition, the dust removal rate in each step of the clothing care program was analyzed to investigate the effects of heat, moisture, and mechanical actions on PM removal.

2 Experimental

2.1 Materials

Six fabrics woven or knitted of cotton, wool, or polyester fibers were prepared, as shown in Table 1.

Test dust particles (ISO 12103–1, A2 fine test dust), with yellowish color like that of fine dust, were applied to each prepared sample to create dusty fabric with PM (DF); Tables 2, 3 show their chemical compositions and particle size distributions, respectively. For uniform and reproducible adhesion of PM, a cabin air filter system (PAF 111, Topas GmbH, Germany) that can cause the airborne adhesion of PM was used. The artificial PM was introduced at the upper filter of the cabin air filter system and descended to the sample surface at a flow rate of approximately 50 m³/h. And the amount of PM attached to samples varied depending on the type of the fabric used; woven cotton 0.113 g, woven polyester 0.302 g, and woven wool 0.226 g.

The digital image processing program Image J (version 1.52a NIH, USA) was used to evaluate the dust removal rate from the sample surface. PM was distinguished from the fabric (yarn and pores) using the brightness values (0–255) of each pixel in images of each sample captured under the

Table 1 Specifications of samples

Sample code	Fiber category	Construction	Weight (g/m ²)	Thickness (mm)	Standard moisture regain (%) [12]
Cw	Cotton (staple)	Woven	125.4	0.2	8
Ck		Knit	184.7	0.4	
Pw	Polyester (filament)	Woven	129.3	0.2	0.4
Pk		Knit	129.1	0.4	
Ww	Wool (staple)	Woven	279.3	0.7	16
Wk		knit	171.6	0.5	

Table 2 Chemical composition of A2 fine test dust

Chemical	% By weight	Chemical	% By weight
Silicon	69.0–77.0	Calcium	2.5–5.5
Aluminum	8.0–14.0	Magnesium	1.0–2.0
Iron	4.0–7.0	Titanium	0.0–1.0
Sodium	1.0–4.0	Potassium	2.0–5.0

Table 3 Cumulative particle size distributions of A2 fine test dust

Size (μm)	Cumulative content (%) by volume
0.97	4.5–5.5
1.38	8.0–9.5
2.75	21.3–23.3
5.50	39.5–42.5
11.00	57.0–59.5
22.00	73.5–76.0
44.00	89.5–91.5
88.00	97.9–98.9
124.50	99.0–100.0
176.00	100.0

same conditions. As shown in Fig. 2, the area in which the brightness distribution of PM overlapped that of the fabric was smaller in the black sample than in the white sample, indicating that the black sample is more effective for distinguishing PM from fabric. Therefore, black fabric samples were used in this study for effectively distinguishing PM from the fabric.

2.2 Clothing care machine

The dust removal function of a commercially available clothing care machine (FAD-01/02, Coway Co. Ltd., Republic of Korea) was used. The dust removal course has four steps, as shown in Table 4; the temperature and humidity conditions inside the machine at each step are shown in Fig. 3.

2.3 Characterization

2.3.1 PM removal rate evaluation

The following three fabrics were used to evaluate the removal rate: unmodified black fabric (BF), DF (dusty fabric with PM), and fabric from which dust was removed by the clothing care machine (RF). The DF was attached to the lower part of the right sleeve of a commercially available

Fig. 2 Overlap in pixels between brightness distributions of PM and white and black fabric samples

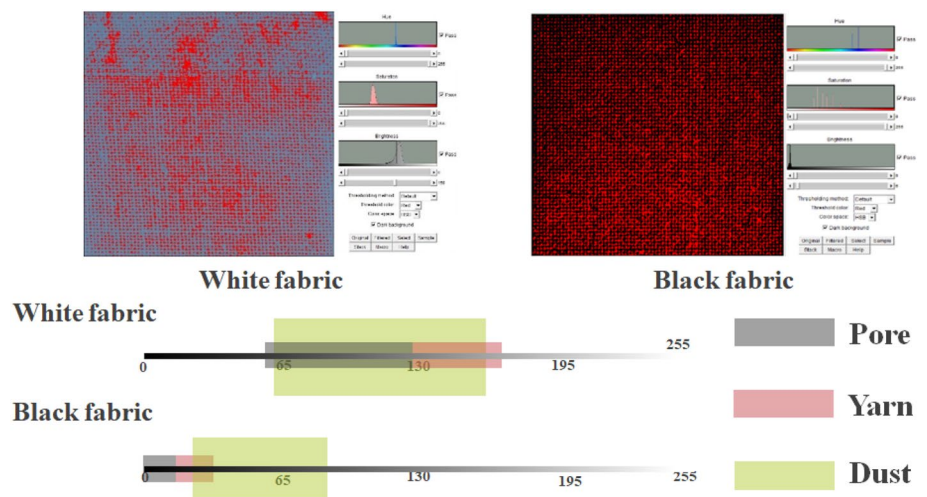
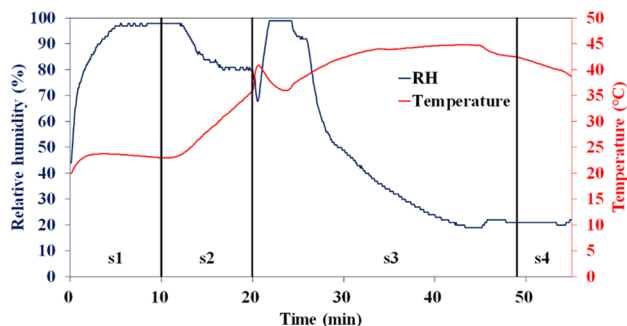


Table 4 Overview and four steps of dust removal course

Code	Configuration	Time (min)
Dust Course	1 cycle (s1 + s2 + s3 + s4)	55
Step 1 (s1)	Low temp. + high humidity + strong air flow	10
Step 2 (s2)	High temp. + high humidity	10
Step 3 (s3)	High temp. + high humidity → high temp. + low humidity	29
Step 4 (s4)	High temp. + low humidity + strong air flow	6

**Fig. 3** Temperature and relative humidity during dust course

dress shirt and was treated using the dust course of the machine, as shown in Fig. 4.

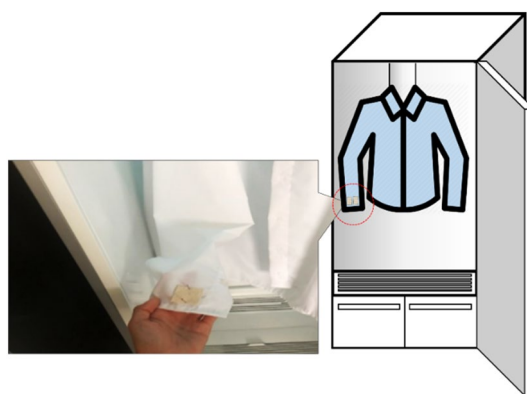
The dust removal rate after treatment by the clothing care machine was evaluated by weighing the samples and using digital image processing.

2.4 Evaluation of PM removal rate of each step

The PM removal rate of each step in the dust removal course (Table 4) was measured to investigate the effect of the environmental conditions in each step. In Step 1, the test was

$$\text{Removalrate(\%)} = \frac{\text{Weight of experimental group DF} - \text{weight of experimental group RF} + K\alpha}{\text{Weight of experimental group DF} - \text{weight of experimental group BF}} \times 100 \quad (2)$$

performed during the first 10 min of the dust course. After Step 1 was complete, the clothing care machine was stopped, and the samples were removed to evaluate the removal rate. When evaluating the removal rates of Steps 2, 3, and 4, to provide the same conditions (humidity, temperature, air current) to the actual cleaning situation, prior stages were first applied to the same shirt without DF. And the machine was paused once it reached the stage in question and the DF was attached to the shirt. Then, the machine was operated continuously for the duration of each step.

**Fig. 4** Photograph of prepared sample and illustration of sample in clothing care machine

2.5 Weight measurement

Samples with dimensions of $100 \times 100 \text{ mm}^2$ were prepared, and the amount of dust removed was calculated as the difference between the weights of the DF and RF. Because PM is very light, the error caused by the moisture regain of the sample after care may significantly affect the experimental results. Therefore, a control group X and an experimental group Y were separately set, and the amount of dust removed by the clothing care machine was calculated using Eq. (1).

Amount of dust removed

$$= \text{weight of experimental group } Y'(DF) - \text{weight of experimental group } Y''(RF) + K\alpha \quad (1)$$

where K is the error between the control and experimental groups, and α is a constant that corrects for the error in weight resulting from changes in the moisture content of the control group in the clothing care machine.

Finally, the dust removal rate was calculated using Eq. (2).

Figure 5 shows a schematic illustration of the PM removal rate evaluation method based on weight measurement (WM).

2.6 Digital image processing

Samples with dimensions of $30 \times 30 \text{ mm}^2$ were prepared, and external images of the BF, DF, and RF were captured, as shown in Fig. 6. A darkroom was prepared by blocking external light sources, and black paper was glued to the inner sides of a lidless $35 \times 37 \times 17 \text{ cm}^3$ cardboard box to minimize

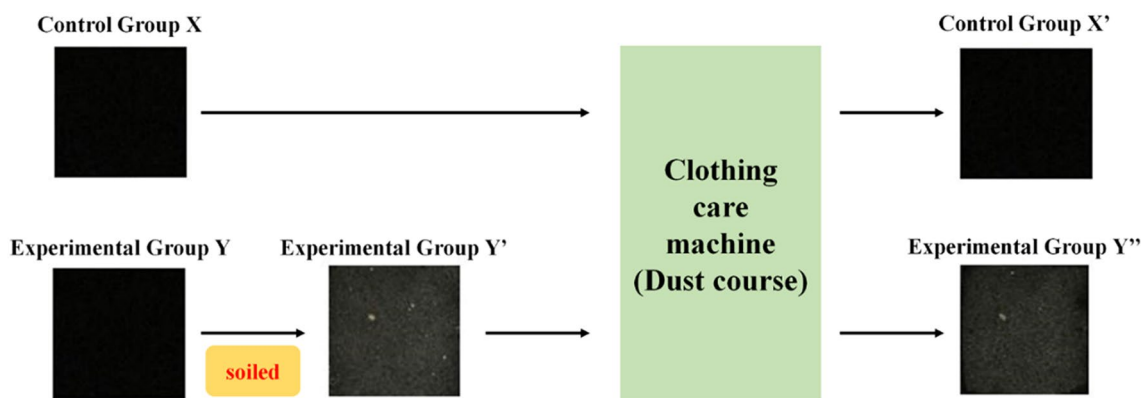


Fig. 5 Illustration of dust removal evaluation by WM method using control group and experimental group

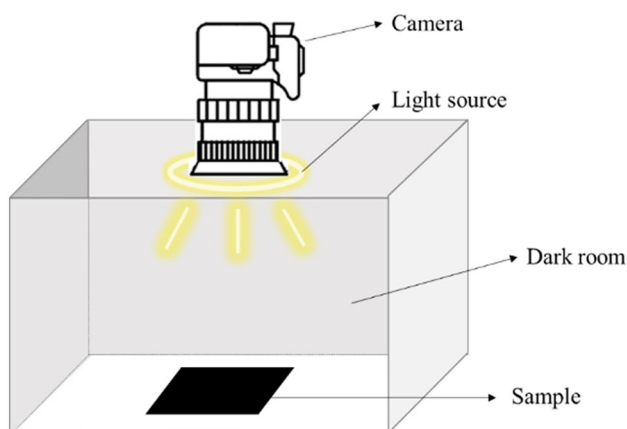


Fig. 6 Conditions for sample imaging

Table 5 Specifications of DSLR and macro ring lite

DSLR	Resolution (pixel)	5472 × 3648
	ISO	ISO 100
	Exposure time (s)	1/100
	F-stop	F/29
Macro-ring lite	Brightness	$\frac{1}{4} < X < \frac{1}{2}$

unnecessary light and reflection. A circular LED light (MR-14EX 2, Canon, Japan) was mounted on the lens (Canon EF 100 mm f/2.8L IS USM Macro Lens, Canon, Japan) of a digital single-lens reflex camera (DSLR, EOS 70D, Canon, Japan). Then, each sample was placed at the bottom of the box, and the camera, which was mounted on a tripod facing the sample, was used to capture an image of its surface.

The distance between the lens and the sample was 25 cm. The light source provided uniform lighting, and the image capture conditions were set so that objective and accurate photograph data could be obtained (Table 5).

The captured images were converted to black-and-white images by changing the weighted RGB value of each pixel to grayscale according to Eq. 3.

$$Gray = 0.299red + 0.587green + 0.114blue \tag{3}$$

Each pixel in the converted images had a brightness intensity between 0 and 255. For each sample image, the number of pixels with each brightness intensity was calculated. Next, the fraction of pixels with each brightness intensity among all the pixels in the image was obtained using Eq. (4). Figure 7(a) shows the pixel distribution rates of the BF, DF, and RF according to the brightness intensity.

Pixel distribution rate of brightness intensity, $x(\%)$

$$= \frac{\text{Number of pixels with brightness intensity } x}{\text{Total number of pixels}} \times 100 \tag{4}$$

Three methods were used to obtain the dust removal rate via digital image processing: the distribution threshold (TH_D) method, cumulative threshold (TH_C) method, and mean brightness value (MBV) method.

In the TH_D and TH_C methods, the minimum brightness intensity considered to represent the presence of dust was selected as a threshold according to different criteria, and all brightness intensity regions above the threshold were identified as dust. The dust removal rate was calculated using the dust distribution rates of the DF and RF [the sum of the pixel distribution rates for the DF and RF corresponding to dust; colored areas in Fig. 7b, c, respectively] according to Eq. (5).

In the TH_D method, the pixel distribution rate of the BF for each brightness intensity was used to determine the threshold. In the pixel distribution rate curve of the BF [Fig. 7a], the brightness intensity at which the distribution rate first becomes 0.05% or less (i.e., 0.0% when rounded) after the peak was identified as the threshold. For the TH_C

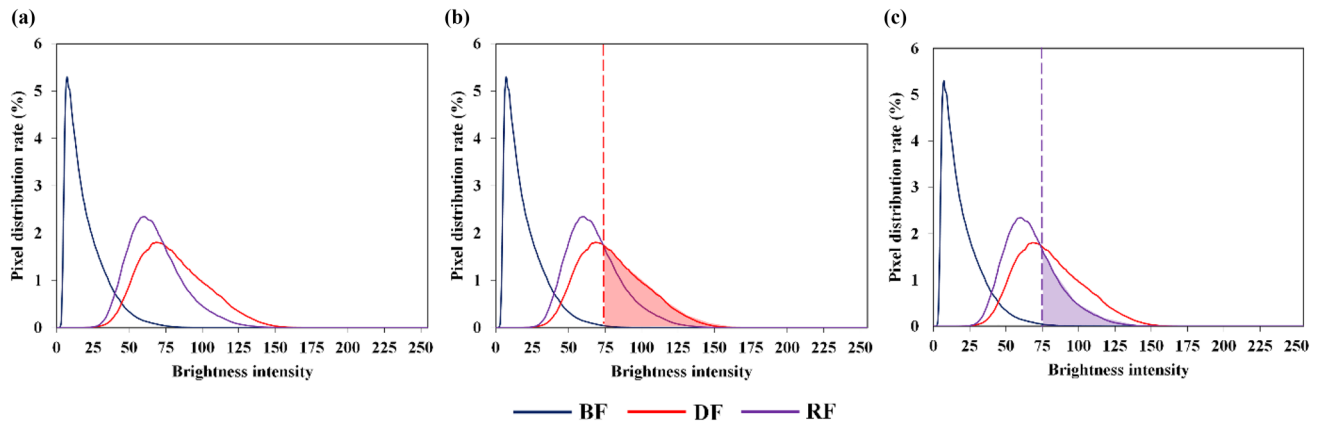


Fig. 7 a Brightness distribution of pixels in images of BF, DF, and RF and fractions identified as dust for b DF and c RF according to the minimum brightness intensity (threshold) considered to represent dust

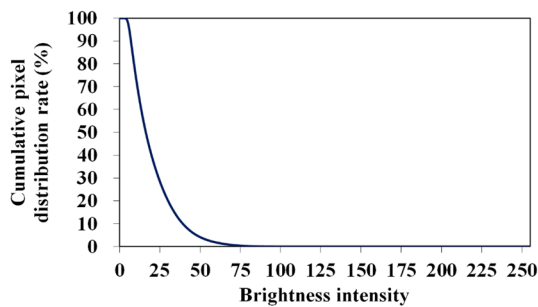


Fig. 8 Cumulative pixel brightness distribution for the BF

method, the cumulative pixel distribution rate, which is the value obtained by accumulating the pixel distribution rate of the BF for each brightness intensity in the opposite direction (brightness intensity $255 \rightarrow 0$), was used to determine the threshold (Fig. 8). The brightness intensity at which the cumulative pixel distribution rate first becomes 0.05% or less while moving from the lowest brightness (0) to the highest brightness (255) (i.e., 0.0% when rounded) was identified as the threshold.

was used. The average brightness intensity was calculated using Eq. (6).

$$B = \frac{\sum_{x=0}^{255} xI_x}{\sum_{x=0}^{255} I_x} \quad (6)$$

where I_x is the number of pixels corresponding to brightness intensity x .

Using the values from the MBV method, which employs the average brightness intensity, the dust removal rate was obtained according to Eq. (7).

$$\text{Dust removal rate}(\%) = \frac{B_{DF} - B_{RF}}{B_{DF} - B_{BF}} \times 100 \quad (7)$$

where B_{BF} is the average brightness intensity of the BF, B_{DF} is the average brightness intensity of the DF, and B_{RF} is the average brightness intensity of the RF.

2.7 Surface properties

To compare the surface properties and dust removal rates of the samples, the surface morphology and friction

$$\text{Dust removal rate}(\%) = \left(1 - \frac{\text{RF dust distribution rate}}{\text{DF dust distribution rate}}\right) \times 100 = \left(1 - \frac{\sum_{x=0}^{255} R_x}{\sum_{x=0}^{255} D_x}\right) \times 100 \quad (5)$$

where x is brightness intensity (0 to 255), D_x is the pixel distribution rate for the brightness intensity x of the DF, and R_x is the pixel distribution rate for the brightness intensity x of the RF.

Finally, for the MBV method, in which the removal rate is calculated without designating a threshold, the average brightness intensity (B) of all pixels in each sample image

properties were measured. A mobile video microscope system (SV-100, Somotech, Korea) was used to observe the surface morphology. An optical lens with a magnification of $160\times$ was attached to the stage viewer, and the focus was adjusted with a fine screw to observe the fabric structure. Images from the video microscope system were captured and saved using the iSolution Lite $\times 64$

software (IMT Inc., USA). Samples were cut into 20×20 cm² specimens, and the coefficient of friction was measured using the Kawabata evaluation system (KES-FB4, Kato Tech, Japan) in the warp (wale) and weft (course) directions. Three tests were performed, and the values were averaged.

3 Results and discussion

3.1 Comparison of dust removal rates obtained using the evaluation methods

To examine the reliability of the removal rate evaluation methods based on digital image processing, their results were compared with the WM results. In previous studies, the washing performance for particulate soil was evaluated by calculating the amount of soil adhesion and removal by measuring the weight of soil compared to the weight of the sample [13, 14]. Here, the removal rate was evaluated using three digital image processing methods (TH_D, TH_C, and MBV) and WM; the results are shown in Fig. 9.

The removal rate for the woven samples was determined by WM to validate the digital image processing methods. The removal rate for all four methods was found to follow the order polyester fabric > cotton fabric > wool fabric. This result confirmed that the three removal rate evaluation methods using digital image processing have a certain level of reliability.

For the TH_D and TH_C methods, in which a threshold was selected, the TH_C method was found to yield higher removal rates than the TH_D method for all samples. The reason is the difference in threshold selection criterion between these methods. In the TH_D method, the brightness intensity at which the distribution rate first becomes 0.05% on the right side of the peak in the PM distribution curve [Fig. 7a] was selected as the threshold. By contrast, in the TH_C method, the brightness intensity at which the

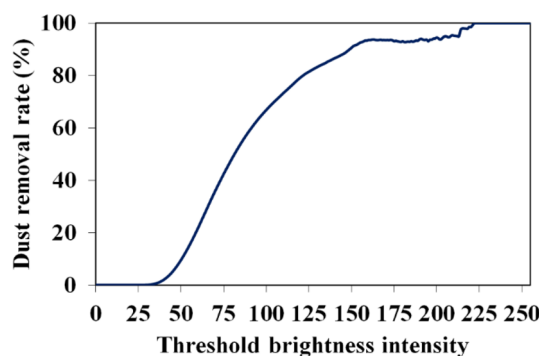


Fig. 10 Dust removal rate as a function of threshold brightness intensity in TH_D and TH_C methods

cumulative pixel brightness distribution rate first becomes 0.05% or less moving in the opposite direction (Fig. 8) was selected as a threshold. Owing to this difference, the threshold values determined using the TH_D method are lower than or equal to those obtained using the TH_C method for all samples. As shown in Fig. 10, the dust removal rate tends to increase as the threshold value of the brightness intensity *x* increases. Therefore, the removal rates determined using the TH_C method were higher than those obtained using the TH_D method.

The TH_D and TH_C methods yielded higher removal rates for the woven samples than for the knitted samples for all fiber types. When the MBV method was used, however, the removal rates were similar for woven and knitted cotton fabrics (Cw, Ck), and the knitted wool sample (Wk) exhibited a higher removal rate than the woven wool sample (Ww).

When dust is removed from a sample, the pixel brightness can change in various ways depending on the threshold α , as shown in Fig. 11. When the dust removal rate was evaluated in this study, the brightness change in Case 1 was not regarded as dust removal. The brightness difference between a3 and a4 is more likely to result from the curvature of the sample rather than a difference in the amount of dust, as only

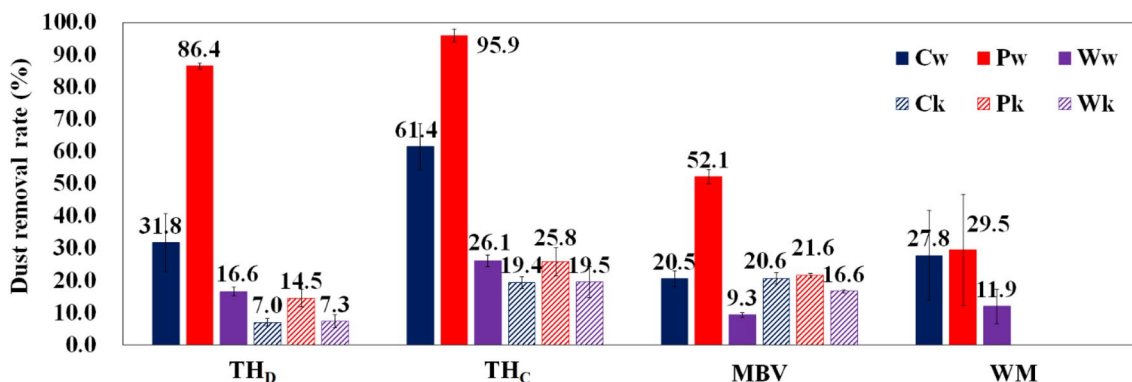


Fig. 9 Dust removal rates obtained by each evaluation method

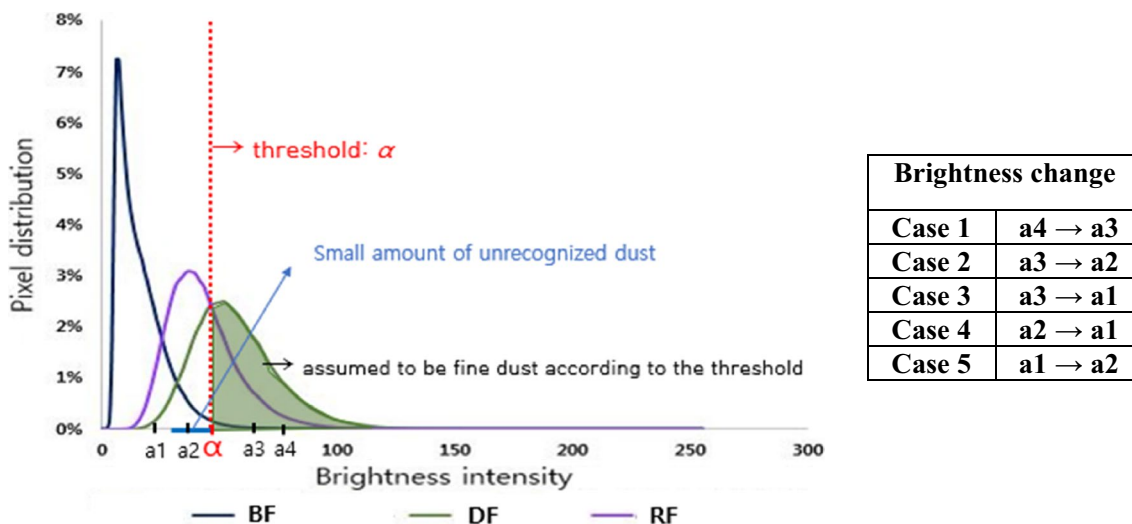


Fig. 11 Various possible changes in pixel brightness during dust removal

a thin layer of dust was applied to the samples in this study. The changes identified as Cases 2 and 3 should have the same interpretation regarding the amount of dust removed. The final brightness of the pixel with values below α , does not affect the removal rate. Cases 4 and 5 were not interpreted as dust removal because these brightness change occurred within a range below the threshold value. These changes might have occurred because of a change in the structure or curvature of the sample, which changed the way samples reflected light after treatment.

When the TH_D and TH_C methods are used, a small amount of fine dust having a brightness within the brightness range of the untreated fabric may not be recognized. However, the TH_D and TH_C methods are relatively accurate because they consider the surface properties of the samples and consider only changes beyond the threshold; thus, Cases 1, 4, and 5 are irrelevant. In addition, if the brightness of any pixel changes from above the threshold to below it, the interpretation is the same for these two methods.

By contrast, when the MBV method is used, no threshold is set, leaving no room for the intervention of a researcher, which leads to a higher likelihood of the results showing consistency when reproduced. In addition, the surface properties of the fabric samples were not considered. Thus, Case 4 can influence the degree of dust removal, which is not the case for the other two methods. When the brightness of a pixel changes from above the threshold to below it, this change will be perceived differently depending on the final brightness of the pixel. For instance, Case 3 is thought to indicate more dust removal than Case 2. By contrast, these two changes have the same interpretation when the TH_D and TH_C methods are used.

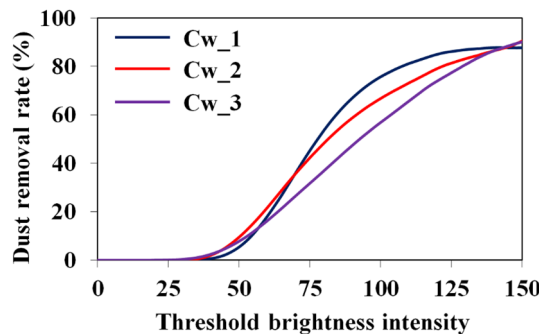


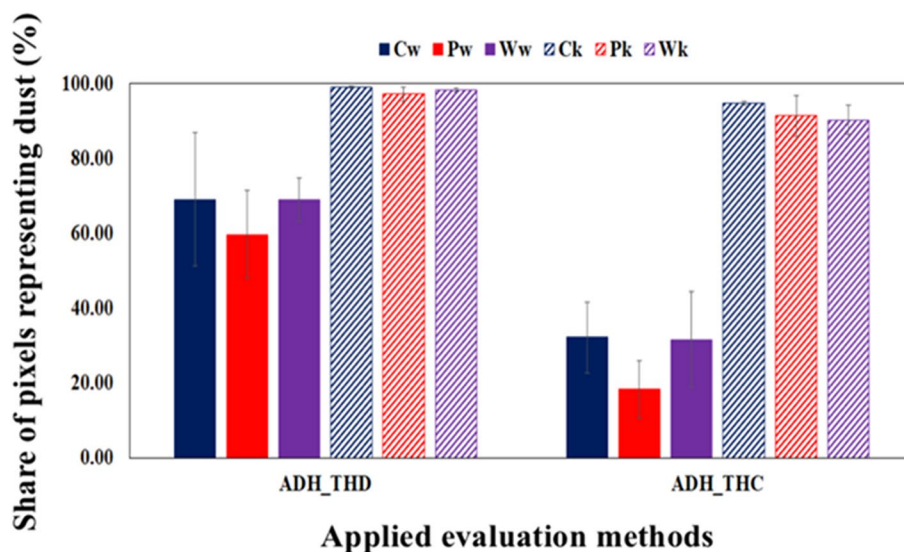
Fig. 12 Rates of dust removal C_w according to the threshold brightness intensity

3.2 Reproducibility of PM removal rate evaluation methods based on threshold selection

Unlike the MBV method, in which the same criterion is applied for all samples, the TH_D and TH_C methods use a different threshold brightness for each sample. Therefore, the reliability of the evaluation methods based on threshold selection was evaluated. Figure 12 shows the removal rates of three different C_w samples according to the threshold brightness intensity.

When the removal rate was calculated using the threshold values based on the brightness intensity obtained by the TH_D and TH_C methods for each sample, as shown in Fig. 12, the dust removal rates were found to be 31.8% ($\pm 8.9\%$) for the TH_C method and 61.4% ($\pm 7.2\%$) for the TH_D method. Consistent removal rates were calculated in repeated experiments,

Fig. 13 Amount of dust adhering to samples



confirming that the removal rate evaluation methods based on digital image processing and threshold selection are accurate and reproducible.

3.3 Effect of material characteristics on the amount of dust adhering to samples

Before the dust removal rate was evaluated, the amount of dust on each type of fabric sample was measured; the results are shown in Fig. 13.

The knit samples contained more dust than the woven samples. This difference is attributed to differences in the surface structures of the samples. Surface roughness decreases the adhesion force between two bodies in contact [15]. That is, large particles adhere strongly to smooth surfaces; accordingly, the contact area and adhesion force will be lower for rough surfaces [16]. However, if the particle size is smaller than the interval of surface roughness, the adhesion force on a particle depends on its location on the surface. Particles that fit into pits or grooves will be

more strongly attracted to the surface, whereas those on bumps and ridges will feel weaker adhesion compared to that on smooth surfaces, as shown in Fig. 14 [17]. Therefore, the adhesion force between the particles and the surface depends on the particle size and surface roughness.

In the cabin air filter system used in this study to expose the samples to PM, air flow carrying dust passes through the upper part of the chamber, where the fabric sample is placed, and is sucked into the lower part. Therefore, the dust in the air moves downward and meets the fiber surface and interfiber or interyarn spaces. Particle adhesion is generally governed by van der Waals, electrostatic, and hydrogen bonding interactions. Although the radius of the dust particles used in this study is larger than that of the fiber, it is smaller than the radius of curvature created by the yarns. Microscopic images of the samples show that the surface structure of the knit fabrics is hairier and looser than that of the woven fabrics. In the woven cotton and polyester samples, the spacing between the yarns is narrow, and the pores are small. Because the

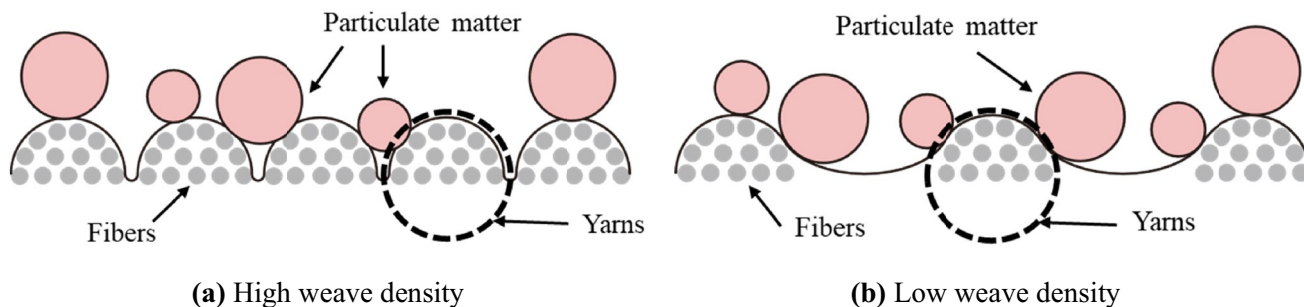
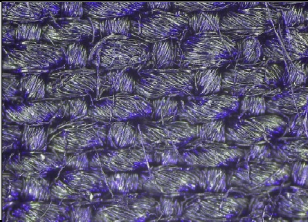
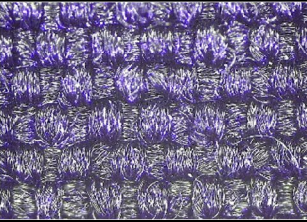
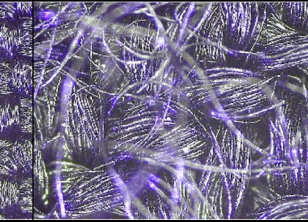
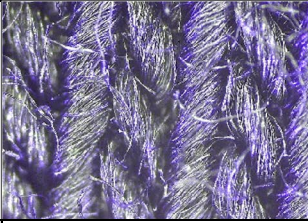
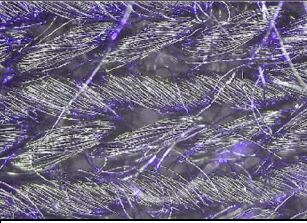



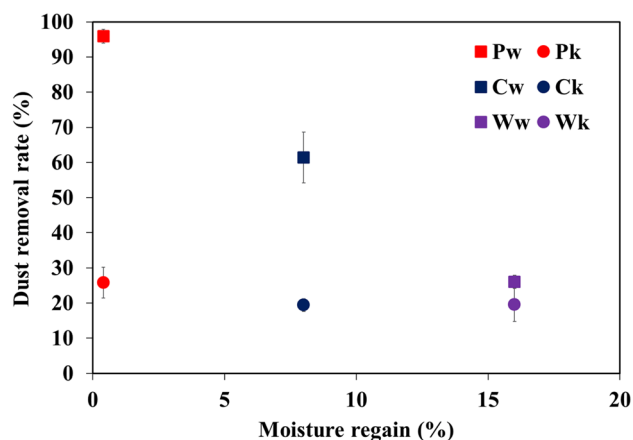
Fig. 14 Schematic showing possible ways that dust particles can adhere to rough substrates with different weave densities

Table 6 Surface image, SMD, and density of samples

Sample	Cw	Pw	Ww
Optical image			
Weave density	143 × 67	117 × 108	66 × 104
SMD (warp/weft)	1.65/1.30	2.36/1.41	4.53/1.86
Sample	Ck	Pk	Wk
Optical image			
Weave density	20 × 44	39 × 41	33 × 62
SMD (wale/course)	1.02/1.51	1.11/1.19	1.79/1.68

woven samples have higher weave density (Table 6), dust particles are less likely to fit into pits or grooves between the yarns. Thus, particles rest on the yarn, which also has a rough surface owing to its fibers. Because the particles have a larger radius than the fibers, the particles rest on bumps and ridges on the yarn. Consequently, the van der Waals force between the yarn and a particle is weaker, and fewer particles adhere to the fabric. By contrast, the knitted samples had comparatively large pores and free fibers floating above the surface. Because yarns in the knitted fabrics form loops, they can move freely, and fine fibers are pulled from the yarns, making them hairy and bulky [18]. Because the knitted samples had lower weave density, dust particles were more likely to land on pits and grooves, where they are most strongly attracted to the fabric. As a result, particles exhibited greater adhesion on the knitted fabrics than on the woven samples.

In addition, hairy surfaces are thought to provide additional surface area for dust adhesion on the surface or in the inner spaces, as the knitted samples, which have hairier surfaces and more free fibers, showed higher dust adhesion. The effect of surface hairiness was more

**Fig. 15** Dust removal rate of samples versus moisture regain

pronounced in the woven fabrics. Fewer particles adhered to the polyester fabric, which was composed of filament yarns, than to the cotton and wool fabrics woven with staple yarns.

3.4 Effect of material characteristics on removal rate

3.4.1 Dust removal rate depending on moisture regain of the fiber

Among the fiber types, polyester had the highest removal rate according to all the evaluation methods, followed by cotton; the removal rate (obtained by the TH_C method) versus moisture regain is plotted in Fig. 15. The removal rate tends to be inversely proportional to the standard moisture regain of the fiber. As the moisture regain of the fiber decreases, electric charges easily accumulate on the surface, increasing chargeability. Hydrophobic fibers with low moisture regain, such as polyester fibers, exhibit higher chargeability than hydrophilic fibers with high moisture regain, such as cotton and wool fibers. Getchell [5] found that PM can be retained if there is bonding energy, including electrostatic attraction, between PM and the fiber surface. Thus, dust adheres more easily to fibers with high chargeability due to electrostatic attraction. During treatment by the clothing care machine, the relative humidity inside the machine sometimes exceeds 90% because of humidification, and moisture is adsorbed

on the fibers. Therefore, the moisture regain and electrical conductivity of the polyester fibers increase simultaneously, discharging the electric charges accumulated on the surface. Consequently, the bonding force between the polyester fibers and PM caused by electrostatic attraction decreased, and the PM was effectively removed by the clothing care machine.

In fibers with high moisture regain, such as cotton and wool, PM that adhered in the airborne state comes into contact with moisture when the humidity of the surrounding environment increases. According to Compton [19], PM components dissolved in liquids can penetrate deeply through pores in the swollen fibers. In addition, the PM that penetrates the fibers adheres strongly to the interior of the fibers through hydrogen bonds and electrostatic attraction and thus becomes waterborne [5]. The lower dust removal rates of cotton and wool compared to polyester are attributed to the increase in the bonding energy of the PM on them as the PM became waterborne in the high-humidity section of the treatment process.

3.5 Dust removal rate depending on geometrical structure of samples

The removal rate of the woven samples was found to be higher than that of the knitted samples, as shown in Fig. 16

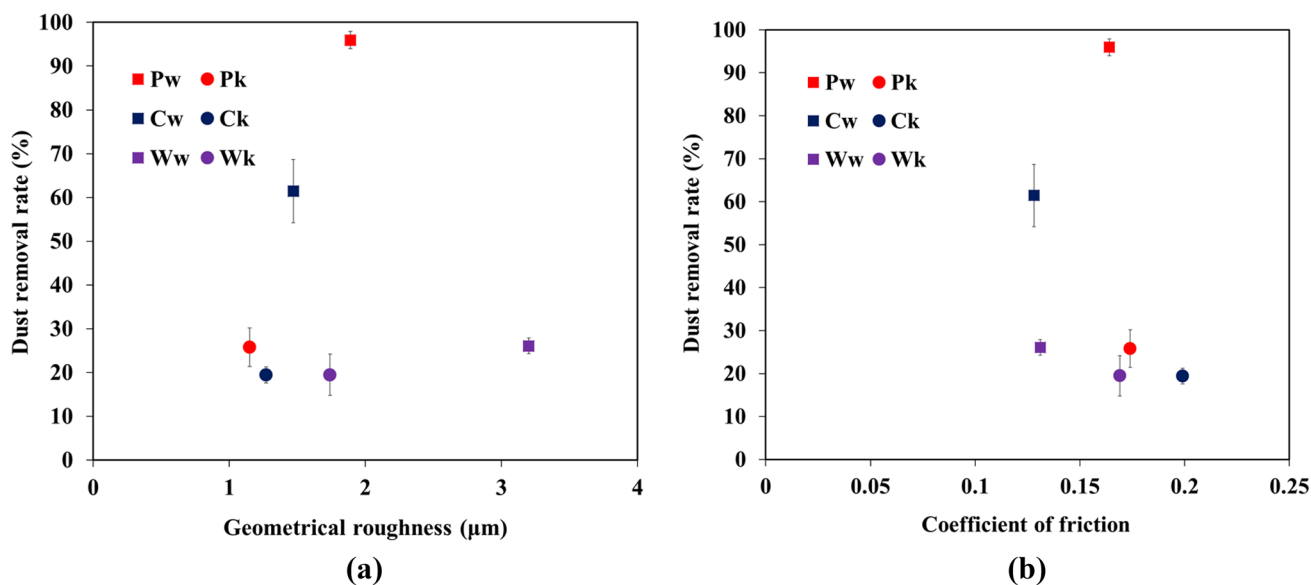


Fig. 16 Dust removal rate versus a surface roughness and b coefficient of friction

Table 7 Friction coefficients of samples

Sample	Cotton		PET		Wool	
	Cw	Ck	Pw	Pk	Ww	Wk
warp/wale	0.128	0.197	0.157	0.168	0.129	0.17
weft/course	0.127	0.201	0.17	0.18	0.133	0.167
Average	0.128	0.199	0.164	0.174	0.131	0.169

Bold indicates the average values

(a). This behavior is attributable in part to the effects of surface roughness on particle adhesion. Dust particles were weakly bonded to the woven cotton and polyester samples because of the high surface roughness and weave density, and thus the dust removal rate was high. In the woven wool sample, the hairy surface offset the effect of high weave density by creating spaces between the yarns for dust to penetrate. The opposite was true of the knitted samples.

The coefficient of friction also depends on the fabric structure. The removal rate was analyzed in terms of the coefficient of friction of each sample. The average friction coefficient and surface roughness in the warp and weft (or wale and course) directions of each sample are listed in Table 7. Figure 16 (b) shows the dust removal rate (obtained by the TH_C method) versus the coefficient of friction. The woven samples, which had low coefficients of friction, had higher removal rates than the knitted samples. Thus, it can be assumed that the dust removal rate is inversely proportional to the coefficient of friction of the clothing material. When the removal rates were compared on the basis of the coefficient of friction regardless of fiber type, the samples with a coefficient of friction between 0.165 and 0.18 (Pk, Ck, and Wk) showed low removal rates of 30% or less, whereas those that had a low coefficient of friction (between 0.10 and 0.165; Pw and Cw) had high removal rates (95.9% and 61.4%, respectively), confirming that the coefficient of friction is an important factor affecting the dust removal rate.

To remove PM from a sample, physical force must be applied, and this force must exceed the frictional force or adhesive force. Surfaces with a high coefficient of friction are generally known to have high adhesive properties [18, 20]. In the clothing care machine, a mechanical force is applied to the sample by air flow. Under the combined application of frictional and adhesive forces, it appears that the separation of PM was relatively difficult for samples with high coefficients of friction. And it appears in figure that dust removal rate is generally inversely

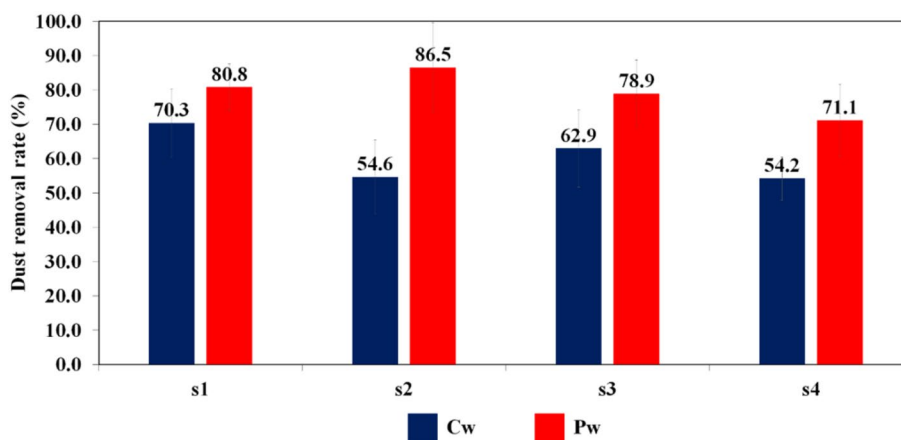
proportional to the coefficient of friction, except for Pw sample. This outlying sample presents how the removal rate is affected by several factors—moisture gain and other surface characteristics—interacting with one another. Considering the relatively low removal rate of Pk which has similar moisture regain and coefficient of friction as Pw but low geometrical roughness, geometrical roughness seems to be the reason behind the high removal rate of Pw.

3.6 Dust removal rate according to conditions in clothing care machine

To examine the dust removal rate according to the environmental conditions in the clothing care machine, the dust removal rate (obtained by the TH_C method) of the Cw and Pw samples was evaluated for each step (s1–s4) of the dust course of the machine. The results are shown in Fig. 17.

The dust removal rate varied with air flow and humidity in the clothing care machine. The dust removal rate of Cw was highest in Step 1, followed by Steps 3, 2, and 4. For Pw, however, the dust removal rate was highest in Step 2, followed by Steps 1, 3, and 4. Step 2 is a very humid segment of the process, and the relative humidity in the clothing care machine is maintained at 70% or higher during the entire period (Fig. 3). A large amount of dust adhered to the polyester fibers owing to electrostatic attraction caused by the low moisture regain, as described above. Accordingly, in Step 2, it appears that dust was easily removed owing to the loss of electrostatic attraction, as high environmental humidity was maintained during the entire period. For Cw, the removal rate appears to have been relatively low in Step 2 because dust had adhered in the waterborne state. In Step 1, however, where the relative humidity was rather low and increased slowly during the process (Fig. 3), Cw had the highest removal rate. The reason is thought to be that a large amount of PM was removed by the action of air flow in the initial section before the relative humidity increased. In addition, in Step 4, both Cw and Pw had the lowest removal

Fig. 17 Dust removal rates in each step of dust course



rates. Step 4 involves dry treatment at a high temperature and very low relative humidity.

4 Conclusion

Objective PM removal rate evaluation methods with high precision and accuracy were developed using digital image processing to evaluate the dust removal performance of clothing care machines. Woven or knitted fabrics of cotton, wool, or polyester fibers were used to analyze the effect of material characteristics on PM removal. In addition, the dust removal rate for each step in the dust function of the clothing care machine was analyzed according to temperature and humidity changes and the presence of air flow in each step. Objective thresholds were set in the TH_D and TH_C methods by analyzing the distribution rate of pixel brightness intensity and the cumulative pixel distribution rate in an image of the untreated samples, and the developed methods were found to have high reliability. Among the fiber types, the polyester samples had the highest removal rates. The reason is thought to be that electrostatic attraction between the polyester fibers and PM was decreased by moisture conditions during the care program, which discharged the electric charges that had accumulated on the surface. Among the fabric structures, woven fabric samples had higher removal rates than knitted fabric samples. It was shown that dust removal depends on the friction coefficient and that samples with high coefficients of friction had low removal rates. The dust removal rate varied in each step depending on the moisture characteristics of the material, confirming that it is necessary to change the course of the clothing care machine depending on the material. This study is significant because it presents methods for the objective and quantitative evaluation of the removal rate of dust adsorbed on fabric surfaces using noncontact image analysis.

Acknowledgements This work was supported by Coway Co., Ltd. (Grant number 0668-20180150)

Data availability The authors declared no potential conflicts of interest with respect to the research, authorship, and/or publication of this article.

Declarations

Conflict of interest The authors declared no potential conflicts of interest with respect to the research, authorship, and/or publication of this article.

References

1. World Health Organization. (2016). Ambient air pollution: A global assessment of exposure and burden of disease.
2. V.P. Aneja, B. Wang, D.Q. Tong, H. Kimball, J. Steger, *JA&WMA* **56**, 1099–1107 (2006)
3. S. Zhang, W.S. Shim, J. Kim. *Mater. Des.* **30**, 3659–3666 (2009)
4. P. Bulejko, *Nanomaterials* **8**, 447 (2018)
5. N.F. Getchell, *Text Res J* **25**, 150–194 (1955)
6. J. Bouloton, T.H. Morton, *J. Soc. Dye. Colour.* **56**, 145–159 (1940)
7. C.M. Hunt, R.L. Blaine, L. Raymond, J. Rowen, W. John, *Text Res J* **20**, 43–50 (1950)
8. J. Compton, W.J. Hart, *Ind. Eng. Chem. Res.* **43**, 1564–1569 (1951)
9. W.T.O. Van, H.A. Endres, *ASH&VE J Sect Heat Pip Air Condit* **24**, 157 (1952)
10. P.A. Florio, E.P. Mersereau, *Text Res J* **25**, 641–649 (1955)
11. S. Choi, Y.J. Hwang, H.J. Lee, M.K. Kim, S.G. Kim, H.S. Kim, *Text Sci Eng* **55**, 89–94 (2018)
12. D. Wilson, *J. Text. Inst.* **54**, T97–T105 (1963)
13. M.H. Mun, I.S. Kang, *J Korean Soc Cloth* **34**, 653–662 (2010)
14. E.K. Roh, H. Ryu, J. Chae, *J Korean Soc Cloth* **41**, 341–351 (2017)
15. S. Rajupet, M. Sow, D. Lacks, *Phys. Rev. E* **102**, 012904 (2020)
16. B. Thomas, O. Klaus, T. Torsten, L. Win, S. Eckhard, *Particles on surfaces: detection. Adhesion and Removal* **9**, 211–223 (2006)
17. H. Mizes, *J Adhes* **51**, 155–165 (1995)
18. B. Emilie, L. Maryline, *Text Res J* **77**, 387–396 (2007)
19. J. Compton, W.J. Hart, *Text Res J* **24**, 263–264 (1954)
20. C.A. Bowers, G. Chantrey, *Text Res J* **39**, 1–11 (1969)

Springer Nature or its licensor (e.g. a society or other partner) holds exclusive rights to this article under a publishing agreement with the author(s) or other rightsholder(s); author self-archiving of the accepted manuscript version of this article is solely governed by the terms of such publishing agreement and applicable law.